Journal of Science and Technology in Civil Engineering, HUCE, 2023, 17 (3): 128–139

DYNAMIC FINITE ELEMENT MODELING OF AXIALLY FUNCTIONALLY GRADED TIMOSHENKO MICROBEAMS UNDER A MOVING MASS

Vu Thi An Ninh[a,*], Nguyen Thi Kim Khue[a]

[a]*Faculty of Basic Sciences, University of Transport and Communications, 3 Cau Giay Street, Dong Da District, Hanoi, Vietnam*

Article history:
Received 14/4/2023, Revised 21/5/2023, Accepted 01/6/2023

Abstract

This paper presents a finite element model for dynamic analysis of axial functionally graded (AFG) microbeams subjected to a moving mass. The material properties of the microbeams are considered to vary in the axial direction by a power-law function, and they are evaluated by Mori-Tanaka scheme. The first-order shear deformation theory is employed in conjunction with the modified couple stress theory to establish the differential equations of motion for the AFG microbeams. A two-node beam element with six degrees of freedom was derived and used in combination with Newmark method to solve the equations of motion and to compute the dynamic response of the microbeams. Numerical investigations are carried out on AFG microbeam with simply supported ends. The proposed method is validated by comparing with results in previous work. The effects of dimensionless material length scale parameters, the material distribution and the moving mass parameters on the dynamic characteristics of the AFG microbeams are studied and discussed in detail.

Keywords: AFG microbeam; dynamic response; modified couple stress theory; finite element model; moving mass.

https://doi.org/10.31814/stce.huce2023-17(3)-10

1. Introduction

Microbeams are widely applied in biosensors, atomic force microscopes, microactuators, and micro-electro-mechanical (MEMS) [1]. In these applications, the microbeams may carry microparticles attaching or moving along the microbeams. For example, integrated complementary metal oxide semiconductor (CMOS)-MEMS free-free beam resonator arrays, AFM probes, and micro/nano scale sensors such as micro accelerometers. Thus, the different behaviors of the microbeam should be evaluated. The classical continuum mechanics theories, however cannot predict the size-dependent behaviors occurring in microbeams due to the lack of material length scale parameters. The modified couple stress theory (MCST), which is a higher-order continuum theory proposed by Yang et al. [2], contains only one material length scale parameter, is widely used in studying the behaviour of microbeams. The use of MCST in evaluating behaviour of homogeneous microbeams has been described in [3–5].

Functionally graded (FG) material is a new type of composite material in which the material properties vary continuously and smoothly from one surface to another. The introduction of FG material has overcome the limitations of traditional composites such as cracking, delamination and stress concentration. With the development of manufacturing technology, the concept of FG material is also extended to microbeams. Many investigations on static and dynamic analyses of FG microbeams have

*Corresponding author. *E-mail address:* vuthianninh@utc.edu.vn (Ninh, V. T. A.)

been reported recently. Ke and Wang [6] studied the dynamic stability of FG microbeams on the basis of the MCST and Timoshenko beam theory. In their study, the material properties are considered to vary in the thickness direction and they are estimated through Mori-Tanaka scheme. Şimşek and Reddy [7] examined the static bending and free vibration of FG microbeam using the MCST and various higher order beam theories. Timoshenko beam theory was used in combination with the MCST by Nateghi and Salamat-talab [8] to study the thermal effect on buckling and free vibration behaviour of FG microbeams. Based on the MCST and Timoshenko beam theory, Ansari et al. [9] solved the free vibration problem of simply supported FG microbeams via the Navier solution.

The moving load problem is of interest to many researchers because of its wide application. Olsson [10] presented the dynamic problem of the homogeneous beam under a moving load based on Euler-Bernoulli beam theory. Both the analytical method and the finite element method were adopted in the study. Wu [11] investigated the dynamic response of an inclined beam due to moving loads by considering each moving load as a moving mass element. Gan et al. [12] used the finite element method to study the dynamic response of AFG Timoshenko beams with non-uniform cross sections under multiple moving forces. In their paper, the material properties of the beam varied continuously in the axial direction according to the power-law function, and they were evaluated by Voigt model. Şimşek et al. [13], Ebrahimi-Mamaghani et al. [14] adopted Euler-Bernoulli beam theory to model the forced vibration of AFG beams under a moving load. The Rayleigh-Ritz method was employed in conjunction with the differential quadrature method by Khalili et al. [15] to obtain the dynamic behavior of an FG beam subjected to a moving load. Vibration of bi-dimensional functionally graded Timoshenko beams under a moving load was studied by Nguyen et al. [16] using the finite element method and Newmark method. The effects of moving load and mass on the dynamic response of the FG beam were studied by Esen et al. [17], also using finite element formulation. Esen et al. [18] proposed a modified continuum mathematical model to investigate the dynamic behaviour of Timoshenko perforated microbeams under a moving load. The effects of moving load and the microstructure size parameter on the dynamic behavior were investigated in detail in their study.

In this paper, the MCST is used in combination with the first-order shear deformation beam theory to study the dynamic response of AFG microbeams under a moving mass. The material properties of the microbeam are considered to vary in the axial direction according to a power-law function, and they are evaluated by Mori-Tanaka scheme. The differential equations of motion of the AFG microbeams are established via Hamilton's principle. A finite element model is developed and used in conjunction with Newmark method to solve the differential equations and to obtain the dynamic response of a simply supported AFG microbeam. The effects of the material length scale parameter, the material distribution, the moving mass speed as well as the mass ratio on the dynamic characteristics of the AFG microbeam are examined in detail.

2. Theory and formulation

A simply supported AFG microbeam of thickness h and width b under a moving mass m, as shown in Fig. 1, is considered. It is assumed that the mass m moves with a constant velocity $v$from the left end to the right end of the beam and it is always in contact with the beam. The Cartesian coordinate system (x, y, z) is chosen such that the x-axis is on the mid-plane, the z-axis is perpendicular to the mid-plane and it directs upward. x_m is the abscissa of the moving mass measured from the left end of the beam.

The microbeam is made from a mixture of ceramic and metal with their volume fractions varying in the axial direction according to [13]

$$V_c(x) = \left(1 - \frac{x}{L}\right)^n; \quad V_m(x) = 1 - V_c(x) \tag{1}$$

where L is the beam length; V_c and V_m are, respectively, the volume fraction of ceramic and metal; n is the power-law index; The subscript 'c' and 'm' in Eq. (1) and hereafter stand for ceramic and metal, respectively.

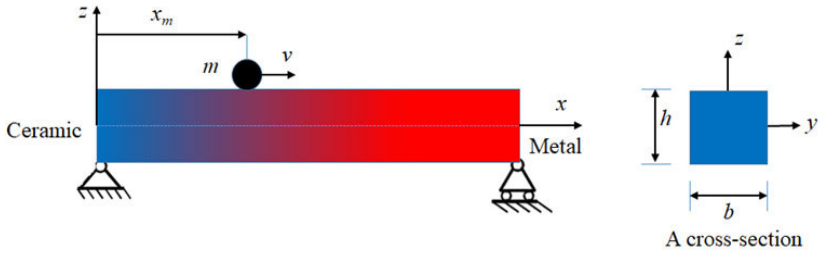

Figure 1. A simply supported AFG microbeam under a moving mass

According to Mori-Tanaka scheme [19], the effective Young's modulus E_f and Poisson's ratio ν_f of the microbeam can be calculated in the form

$$E_f(x) = \frac{9K_fG_f}{3K_f + G_f}; \quad \nu_f(x) = \frac{3K_f - 2G_f}{6K_f + 2G_f} \tag{2}$$

where the effective local bulk modulus K_f and the shear modulus G_f are given by

$$K_f = K_m + \frac{(K_c - K_m)\,V_c}{1 + \dfrac{V_m\,(K_c - K_m)}{K_m + 4G_m/3}}; \quad G_f = G_m + \frac{(G_c - G_m)\,V_c}{1 + \dfrac{V_m\,(G_c - G_m)}{G_m + \dfrac{G_m\,(9K_m + 8G_m)}{6\,(K_m + 2G_m)}}} \tag{3}$$

where $K_i = E_i/[3\,(1 - 2\upsilon_i)], G_i = E_i/[2\,(1 + \upsilon_i)], (i = c, m)$. The effective mass density is defined by Voigt model as

$$\rho_f(x) = \rho_c V_c(x) + \rho_m V_m(x) \tag{4}$$

According to the modified couple stress theory (MCST) [2], the strain energy U of the microbeam can be written as

$$U = \frac{1}{2}\int_V (\boldsymbol{\sigma} : \boldsymbol{\varepsilon} + \mathbf{m} : \boldsymbol{\chi}) dV \tag{5}$$

where V is the beam volume; $\boldsymbol{\sigma}$ and $\boldsymbol{\varepsilon}$ are, respectively, the stress and strain tensors; $\mathbf{m}$ is the deviatoric part of the couple stress tensor; $\boldsymbol{\chi}$ is the symmetric curvature tensor. These tensors are given by [4]

$$\begin{aligned} &\boldsymbol{\sigma} = \lambda\,\mathrm{tr}(\boldsymbol{\varepsilon})\mathbf{I} + 2\mu\boldsymbol{\varepsilon}; \quad \boldsymbol{\varepsilon} = \frac{1}{2}\left[\nabla\mathbf{u} + (\nabla\mathbf{u})^T\right] \\ &\boldsymbol{\chi} = \frac{1}{2}\left[\nabla\boldsymbol{\theta} + (\nabla\boldsymbol{\theta})^T\right]; \quad \boldsymbol{\theta} = \frac{1}{2}\,\mathrm{curl}\mathbf{u}; \quad \mathbf{m} = 2l^2\mu\boldsymbol{\chi} \end{aligned} \tag{6}$$

where $\mathbf{u}$ is the displacement vector; $\boldsymbol{\theta}$ is the rotation vector; $\lambda = \dfrac{E_f\nu_f}{(1 + \nu_f)(1 - 2\nu_f)}$ and $\mu = \dfrac{E_f}{2(1 + \nu_f)}$ are Lame's constants, in which E_f and ν_f are defined in Eq. (2); l is a material length scale parameter.

Based on the first order shear deformation beam theory, the axial and transverse displacements, $u_x\,(x, z, t)$ and $u_z\,(x, z, t)$, respectively of an arbitrary point in the beam are given by

$$\begin{aligned} u_x(x, z, t) &= u(x, t) - z\theta(x, t) \\ u_z(x, z, t) &= w(x, t) \end{aligned} \tag{7}$$

where $u(x,t)$ and $w(x,t)$ are, respectively, the axial and transverse displacements of the point on the mid-plane; $\theta(x,t)$ is the rotation of the cross-section; t is the time variable;

Using Eq. (7), the tensors in Eq. (6) are rewritten as

$$\boldsymbol{\varepsilon} = \begin{bmatrix} \varepsilon_{xx} & 0 & \varepsilon_{xz} \\ 0 & 0 & 0 \\ \varepsilon_{zx} & 0 & 0 \end{bmatrix}; \quad \boldsymbol{\sigma} = \begin{bmatrix} \sigma_{xx} & 0 & \sigma_{xz} \\ 0 & \sigma_{yy} & 0 \\ \sigma_{zx} & 0 & \sigma_{zz} \end{bmatrix}; \quad \boldsymbol{\chi} = \begin{bmatrix} 0 & \chi_{xy} & 0 \\ \chi_{yx} & 0 & 0 \\ 0 & 0 & 0 \end{bmatrix}; \quad \mathbf{m} = 2l^2\mu\boldsymbol{\chi} \tag{8}$$

where

$$\begin{aligned} &\varepsilon_{xx} = u_{,x} - z\theta_{,x}\,; \quad \varepsilon_{xz} = \varepsilon_{zx} = \frac{1}{2}(w_{,x} - \theta) \\ &\sigma_{xx} = (\lambda + 2\mu)\varepsilon_{xx}; \quad \sigma_{xz} = \sigma_{zx} = 2\psi\mu\varepsilon_{xz}; \quad \sigma_{yy} = \sigma_{zz} = \lambda\varepsilon_{xx} \\ &\chi_{xy} = \chi_{yx} = \frac{1}{4}(-w_{,xx} - \theta_{,x}) \end{aligned} \tag{9}$$

where ψ is the shear correction coefficient, equals to 5/6 for the beam with rectangular cross section considered herein.

Using Eq. (8), the strain energy of the microbeam in Eq. (5) can be written in the form

$$\begin{aligned} U &= \frac{1}{2}\int_0^L \int_A \left(\sigma_{xx}\varepsilon_{xx} + 2\sigma_{xz}\varepsilon_{xz} + 2m_{xy}\chi_{xy}\right) dA dx \\ &= \frac{1}{2}A\int_0^L \left[(\lambda + 2\mu)\left(u_{,x}^2 + \frac{h^2}{12}\theta_{,x}^2\right) + \psi\mu\,(w_{,x} - \theta)^2 + \frac{l^2\mu}{4}\,(w_{,xx} + \theta_{,x})^2\right] dx \end{aligned} \tag{10}$$

where $A = b \times h$ is the cross-sectional area of the beam.

The kinetic energy T of the beam is defined as

$$T = \frac{1}{2}\int_0^L \int_A \rho_f(x)(\dot{u}_x^2 + \dot{u}_z^2) dA dx \tag{11}$$

In Eq. (11), an over dot is used to denote the derivative with respect to the time variable. Substituting Eq. (7) into Eq. (11), the kinetic energy of the beam can be rewritten in the form

$$T = \frac{1}{2}A\int_0^L \rho_f(x)\left[(\dot{u}^2 + \dot{w}^2) + \frac{h^2}{12}\dot{\theta}^2\right] dx \tag{12}$$

The potential energy due to moving mass is given by [18]

$$V_m = -\int_0^L \left[\left(mg - m\ddot{w} - 2mv\dot{w}_{,x} - mv^2 w_{,xx}\right) w(x,t) - m\ddot{u}u(x,t)\right] \delta(x_m - vt)\, dx \tag{13}$$

where g is the gravity acceleration; $m\ddot{u}$ and $m\ddot{w}$ are the axial and transverse inertia forces, respectively; $2mv\dot{w}_{,x}$ and $mv^2 w_{,xx}$ are, respectively, the Coriolis and centrifugal forces; $\delta(.)$ is the Dirac delta function.

Applying Hamilton's principle to Eqs. (10), (12) and (13), the differential equations of motion of AFG microbeam under a moving mass are obtained as follows

$$\begin{aligned}
&\delta u: -A\rho\ddot{u} + A\left[(\lambda+2\mu)\,u_{,x}\right]_{,x} - (m\ddot{u})_{x_m} = 0\\
&\delta w: A\rho\ddot{w} - A\left[\psi\mu\,(w_{,x}-\theta)\right]_{,x} + A\left[\frac{l^2\mu}{4}\,(w_{,xx}+\theta_{,x})\right]_{,xx}\\
&\qquad + \left(m\ddot{w} + 2mv\dot{w}_{,x} + mv^2 w_{,xx}\right)_{x_m} = mg\\
&\delta\theta: -\frac{\rho h^2}{12}\ddot{\theta} + \psi\mu\,(w_{,x}-\theta) + \left[(\lambda+2\mu)\,\frac{h^2}{12}\theta_{,x} + \frac{l^2\mu}{4}\,(w_{,xx}+\theta_{,x})\right]_{,x} = 0
\end{aligned} \tag{14}$$

The finite element method used to solve Eq. (14) will be presented in the next section to analyze the dynamic response of the AFG microbeam.

3. Finite element formulation

A finite element model is developed in this section to solve the equations of motion (14). To this end, the beam is assumed to be divided into a number of two-node beam elements with length l_e. The vector of nodal displacement (**d**) for a generic element contains six components as

$$\mathbf{d} = \left\{\begin{array}{cccccc} u_i & w_i & \theta_i & u_j & w_j & \theta_j \end{array}\right\}^T \tag{15}$$

where u_k, w_k and θ_k $(k = i, j)$ are, respectively, the values of the axial, transverse displacements and rotation θ at the node k; The superscript 'T' denotes the transpose of a vector or a matrix.

The displacement field $\mathbf{u} = \{u \;\; w \;\; \theta\}^T$ inside the element is interpolated from the nodal displacements according to

$$\mathbf{u} = \mathbf{N}\mathbf{d} \tag{16}$$

where **N** is the matrix of interpolation functions with the following form

$$\mathbf{N} = \left[\begin{array}{c} \mathbf{N}_u \\ \mathbf{N}_w \\ \mathbf{N}_\theta \end{array}\right] = \left[\begin{array}{cccccc} N_{u1} & 0 & 0 & N_{u2} & 0 & 0 \\ 0 & N_{w1} & N_{w2} & 0 & N_{w3} & N_{w4} \\ 0 & N_{\theta 1} & N_{\theta 2} & 0 & N_{\theta 3} & N_{\theta 4} \end{array}\right] \tag{17}$$

where N_{u1} and N_{u2} are linear functions, N_{wi} and $N_{\theta i}$ $(i = 1, ..., 4)$ are the solution of the static governing differential equations of a homogeneous Timoshenko beam element obtained by Kosmatka [20], and they are defined as follows

$$N_{u1} = \frac{l_e - x}{l_e}; \quad N_{u2} = \frac{x}{l_e} \tag{18}$$

$$\begin{aligned}
N_{w1} &= \frac{1}{1+\phi}\left[2\left(\frac{x}{l_e}\right)^3 - 3\left(\frac{x}{l_e}\right)^2 - \phi\left(\frac{x}{l_e}\right) + 1 + \phi\right]\\
N_{w2} &= \frac{l_e}{1+\phi}\left[\left(\frac{x}{l_e}\right)^3 - \left(2+\frac{\phi}{2}\right)\left(\frac{x}{l_e}\right)^2 + \left(1+\frac{\phi}{2}\right)\left(\frac{x}{l_e}\right)\right]\\
N_{w3} &= -\frac{1}{1+\phi}\left[2\left(\frac{x}{l_e}\right)^3 - 3\left(\frac{x}{l_e}\right)^2 - \phi\left(\frac{x}{l_e}\right)\right]\\
N_{w4} &= \frac{l_e}{1+\phi}\left[\left(\frac{x}{l_e}\right)^3 - \left(1-\frac{\phi}{2}\right)\left(\frac{x}{l_e}\right)^2 - \frac{\phi}{2}\left(\frac{x}{l_e}\right)\right]
\end{aligned} \tag{19}$$

and

$$N_{\theta 1} = \frac{6}{(1+\phi)\, l_e}\left[\left(\frac{x}{l_e}\right)^2 - \left(\frac{x}{l_e}\right)\right]; \quad N_{\theta 2} = \frac{1}{1+\phi}\left[3\left(\frac{x}{l_e}\right)^2 - (4+\phi)\left(\frac{x}{l_e}\right) + 1 + \phi\right]$$
$$N_{\theta 3} = -\frac{6}{(1+\phi)\, l_e}\left[\left(\frac{x}{l_e}\right)^2 - \left(\frac{x}{l_e}\right)\right]; \quad N_{\theta 4} = \frac{1}{1+\phi}\left[3\left(\frac{x}{l_e}\right)^2 - (2-\phi)\left(\frac{x}{l_e}\right)\right] \tag{20}$$

with $\phi = 12E_mI/(12\psi G_mA)$. It is noted that when the shear rigidity approaches infinity, the polynomials in Eqs. (19) and (20) return to the Hermite polynomials and their derivative, respectively. The element formulated from the polynomials in (19) and (20) is, therefore, free of shear locking. In addition, the convergence of the element based on the polynomials in (19) and (20) is much faster than the conventional element using linear interpolation.

Using the interpolations, the strain energy (U) of the microbeam can be written in the form

$$U = \frac{1}{2}\sum^{nel} \mathbf{d}^T \left(\mathbf{k}_{uu} + \mathbf{k}_{\theta\theta} + \mathbf{k}_{ss}\right)\mathbf{d} \tag{21}$$

where *nel* is the total number of elements used to discrete the beam; $\mathbf{k}_{uu}, \mathbf{k}_{\theta\theta}$ and $\mathbf{k}_{ss}$ are, respectively, the element stiffness matrices stemming from the axial stretching, bending and shear deformation. These matrices are as follows

$$\mathbf{k}_{uu} = A\int_0^{l_e} \mathbf{N}_{u,x}^T (\lambda + 2\mu)\, \mathbf{N}_{u,x} dx; \quad \mathbf{k}_{\theta\theta} = \frac{Ah^2}{12}\int_0^{l_e} \mathbf{N}_{\theta,x}^T (\lambda + 2\mu)\, \mathbf{N}_{\theta,x} dx$$
$$\mathbf{k}_{ss} = A\int_0^{l_e} \left[\psi\mu \left(\mathbf{N}_{w,x} - \mathbf{N}_\theta\right)^T \left(\mathbf{N}_{w,x} - \mathbf{N}_\theta\right) + \frac{l^2\mu}{4}\left(\mathbf{N}_{w,xx} - \mathbf{N}_{\theta,x}\right)^T \left(\mathbf{N}_{w,xx} - \mathbf{N}_{\theta,x}\right)\right] dx \tag{22}$$

The kinetic energy in Eq. (12) can also be written in the form

$$T = \frac{1}{2}\sum^{nel} \dot{\mathbf{d}}^T \left(m_{uu} + \mathbf{m}_{ww} + \mathbf{m}_{\theta\theta}\right)\dot{\mathbf{d}} \tag{23}$$

the element mass matrices in Eq. (23) are defined as follows

$$\mathbf{m}_{uu} = \int_0^{l_e} \mathbf{N}_u^T \rho A \mathbf{N}_u dx; \quad \mathbf{m}_{ww} = \int_0^{l_e} \mathbf{N}_w^T \rho A \mathbf{N}_w dx; \quad \mathbf{m}_{\theta\theta} = \int_0^{l_e} \mathbf{N}_\theta^T \frac{\rho A h^2}{12} \mathbf{N}_\theta dx \tag{24}$$

The potential energy in Eq. (13) is of the form

$$V_m = \sum^{nel} \left(\ddot{\mathbf{d}}^T \mathbf{m}_m \ddot{\mathbf{d}} + \dot{\mathbf{d}}^T \mathbf{c}_m \dot{\mathbf{d}} + \mathbf{d}^T \mathbf{k}_m \mathbf{d} - \mathbf{d}^T \mathbf{f}_m\right) \tag{25}$$

where $\mathbf{m}_m, \mathbf{c}_m$ and $\mathbf{k}_m$ are, respectively, the element mass, damping and stiffness matrices due to the effects of the inertia, Coriolis and the centrifugal forces of the moving mass; $\mathbf{f}_m$ is the time-dependent element nodal load vector generated by moving mass. The expressions for $\mathbf{m}_m, \mathbf{c}_m, \mathbf{k}_m$ and $\mathbf{f}_m$ are as follows

$$\underset{6\times6}{\mathbf{m}_m} = \left[\mathbf{N}_u^T m \mathbf{N}_u + \mathbf{N}_w^T m \mathbf{N}_w\right]_{x_e}; \quad \underset{6\times6}{\mathbf{c}_m} = 2v\left[\mathbf{N}_w^T m \mathbf{N}_{w,x}\right]_{x_e}$$
$$\underset{6\times6}{\mathbf{k}_m} = v^2\left[\mathbf{N}_w^T m \mathbf{N}_{w,xx}\right]_{x_e}; \quad \underset{6\times1}{\mathbf{f}_m} = mg\left[\mathbf{N}_w^T\right]_{x_e} \tag{26}$$

In Eq. (26), the notation $[.]_{x_e}$ means that [.] is evaluated at x_e-the current abscissa of the moving mass with respect to the left node of the element. Note that except for the element under the moving mass, the element matrices $\mathbf{m}_m, \mathbf{c}_m, \mathbf{k}_m$ and the load vector $\mathbf{f}_m$ are zeros for all other elements.

Having element mass and stiffness matrices of the microbeam as well as the element mass, damping, stiffness matrices and load vector due to moving mass, the discrete equation of motion for the AFG microbeam can be written in the form

$$(\mathbf{M} + \mathbf{M}_m)\ddot{\mathbf{D}} + \mathbf{C}_m\dot{\mathbf{D}} + (\mathbf{K} + \mathbf{K}_m)\mathbf{D} = \mathbf{F} \tag{27}$$

where $\mathbf{D}, \dot{\mathbf{D}}$ and $\ddot{\mathbf{D}}$ are, respectively, the global vectors of nodal displacement, velocity and acceleration; $\mathbf{M}$ and $\mathbf{K}$ are structural mass and stiffness matrices obtained by assembling the element mass and stiffness matrices, respectively; $\mathbf{M}_m, \mathbf{C}_m, \mathbf{K}_m$ and $\mathbf{F}$ are, respectively, the global matrices and vector constructed by assembling the matrices $\mathbf{m}_m, \mathbf{c}_m, \mathbf{k}_m$ and $\mathbf{f}_m$ over the elements. Eq. (27) can be solved by the Newmark method. The average acceleration method that ensures unconditional convergence is adopted herein.

4. Numerical results and discussion

Dynamic response of the simply supported AFG microbeam under a moving mass is numerically investigated in this section. To this end, the AFG microbeam with $b = h$, the material length scale parameter $l = 17.6$ μm [6] is considered herein. The beam used in this study includes aluminum (Al) and Silicon carbide (SiC) with their material properties as follows [6, 7, 10]

- $E_m = 70$ GPa, $\rho_m = 2702$ kg/m^3, $\nu_m = 0.3$ for Al.
- $E_c = 427$ GPa, $\rho_c = 3100$ kg/m^3, $\nu_c = 0.17$ for SiC.

For convenience, the following non-dimensional parameters are introduced for the dynamic magnification factor D_d, mass ratio r_m, speed parameter f_v and the dimensionless material length scale parameter η as

$$D_d = \max\left(\frac{w(L/2,t)}{w_{st}}\right); \quad r_m = \frac{m}{\rho_m AL}; \quad f_v = \frac{\pi v}{\omega_1 L}; \quad \eta = \frac{h}{l} \tag{28}$$

where $w_{st} = mgL^3/48IE_m$ is the static deflection of an aluminum beam under a load mg acting at mid-span; ω_1 is the fundamental frequency of the simple supported aluminum microbeam. A uniform increment time step $\Delta t = \Delta T/500$, with ΔT is the total time necessary for the mass to cross the beam, is used for the Newmark method.

First of all, it is important to study the accuracy of the derived beam element. In Table 1, the first three frequency parameters of homogeneous microbeam obtained in the present work are compared with the results calculated by Ke and Wang [6] obtained by the differential quadrature method. As seen from the table, the result obtained by the present method agrees with the result of Ref. [6]. The difference between the present result with that of Ref. [6] may be caused by the different methods used in the two works.

Table 1. Comparison of the first three frequency parameters of homogeneous microbeam with $\eta = 2$ and $L/h = 10$

Mode	Ceramic			Metal		
	Ref. [6]	Present work	Error (%)	Ref. [6]	Present work	Error (%)
1	0.8336	0.8437	−1.21	0.3393	0.3752	−10.58
2	3.2081	3.1199	2.75	1.2914	1.3737	−6.37
3	6.8417	6.3181	7.65	2.7165	2.7510	−1.27

Additionally, the comparison of dynamic magnification factor D_d for AFG macrobeam under a moving load in this paper with that of Şimşek et al. [13] is shown in Fig. 2. The following parameters are used to compute the numerical results in Fig. 2: $P = 100$ kN, $E_m = 210$ GPa, $\rho_m = 7800$ kg/m^3, $\nu_m = 0.3$, $E_c = 390$ GPa, $\rho_c = 3960$ kg/m^3, $\nu_c = 0.3$, $h = 0.9$ m, $b = 0.4$ m, $L = 20$ mm and $\eta = 0$. A very good agreement between the results in the present work with those of Ref. [13] is observed in Fig. 2. Note that the results obtained in Ref. [13] are calculated by using Euler-Bernoulli beam theory.

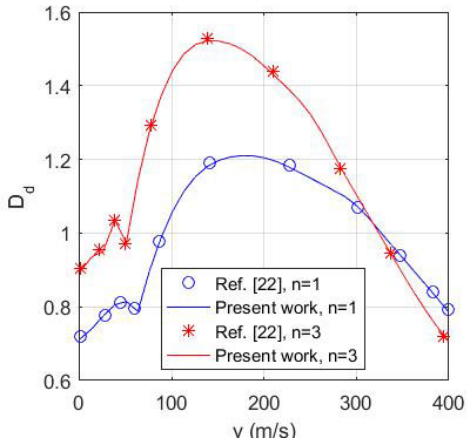

Figure 2. Comparison of dynamic magnification factor for AFG macrobeam ($\eta = 0$) under a moving load

The convergence of beam elements in evaluating the dynamic magnification factor of AFG microbeam is shown in Table 2, where the results obtained by different numbers of the beam elements are calculated for $\eta = 2, L/h = 10, r_m = 0.5, f_v = 0.2$ and various values of the power-law index. As observed from Table 2, convergence is achieved by using 26 elements, regardless of the power-law index. Because of these convergence results, 26 beam elements are used for all the computations reported in the following. Note that the convergence of the results in Table 1 and Fig. 2 has also been achieved by using 26 elements.

Table 2. Convergence of beam element in evaluating dynamic magnification factor of AFG microbeam for $\eta = 2, L/h = 10, r_m = 0.5, f_v = 0.2$

n	$nel = 12$	$nel = 14$	$nel = 16$	$nel = 18$	$nel = 20$	$nel = 22$	$nel = 24$	$nel = 26$
0.5	0.1693	0.1695	0.1696	0.1698	0.1698	0.1696	0.1695	0.1695
1	0.2393	0.2395	0.2396	0.2397	0.2394	0.2394	0.2390	0.2390
2	0.3089	0.3084	0.3082	0.3074	0.3068	0.3074	0.3060	0.3060
5	0.4193	0.4185	0.4174	0.4165	0.4163	0.4150	0.4128	0.4128

Table 3. Dynamic magnification factor of AFG microbeam for $L/h = 10, f_v = 0.1$

r_m	n	η					
		1	2	4	6	8	10
0.25	0.5	0.0693	0.1599	0.2525	0.2843	0.2973	0.3038
	1	0.0973	0.2197	0.3397	0.3813	0.3984	0.4067
	3	0.1653	0.3713	0.5633	0.6246	0.6493	0.6615
0.5	0.5	0.0687	0.1584	0.2490	0.2799	0.2921	0.2984
	1	0.0963	0.2219	0.3476	0.3901	0.4077	0.4160
	3	0.1578	0.3581	0.5434	0.6047	0.6275	0.6392
1	0.5	0.0650	0.1517	0.2450	0.2765	0.2899	0.2964
	1	0.0981	0.2257	0.3520	0.3932	0.4115	0.4194
	3	0.1459	0.3428	0.5307	0.5895	0.6145	0.6280

The dynamic magnification factor D_d of AFG microbeam for $L/h = 10, f_v = 0.1$ and different values of mass ratio ($r_m = 0.25, 0.5, 1$), the power-law index ($n = 0.5, 1, 3, 5$), the dimensionless material length scale parameter ($\eta = 1, 2, 4, 6, 8, 10$) is presented in Table 3. It is clear from Table 3 that factor D_d increases by increasing the index n or decreasing r_m, regardless of parameter η. On the other hand, the influence of parameter η on factor D_d is significant, specifically, increasing η leads to the increase in D_d, irrespectively of n and r_m.

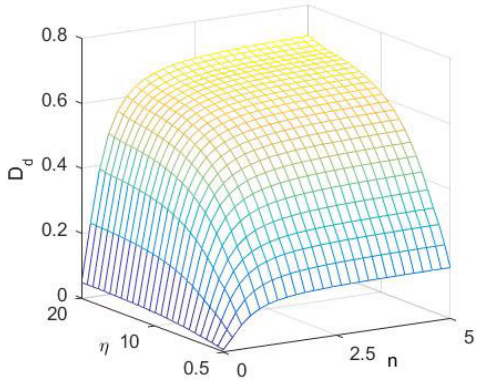

Figure 3. Variation of dynamic magnification factor with power-law index and dimensionless material length scale parameter for $L/h = 20, r_m = 0.5, f_v = 0.1$

The variation of factorD_d with power-law index and dimensionless material length scale parameter is depicted in Fig. 3 for $L/h = 20, r_m = 0.5, f_v = 0.1$. Similar to the results in Table 3, the results in Fig. 3 show that the factor D_d increases with the increase in the power-law index and parameter η.

The effects of the power-law index n and the dimensionless material length scale parameter η on the time histories for mid-span deflection of AFG microbeam are presented in Figs. 4 and 5, respectively, for two values of speed parameter, $f_v = 0.1, 0.3$. Observations from these figures show that the index n and parameter η have a significant effect on the mid-span deflection. The amplitude of the mid-span deflection increases by the increase in the index n and parameter η, regardless of the speed parameter. Besides, the way of vibration of the beam is also highly dependent on the speed parameter, the beam tends to carry out less vibration cycles when the value of the speed parameter is larger, as seen from Figs. 4 and 5, irrespectively of the index n and parameter η.

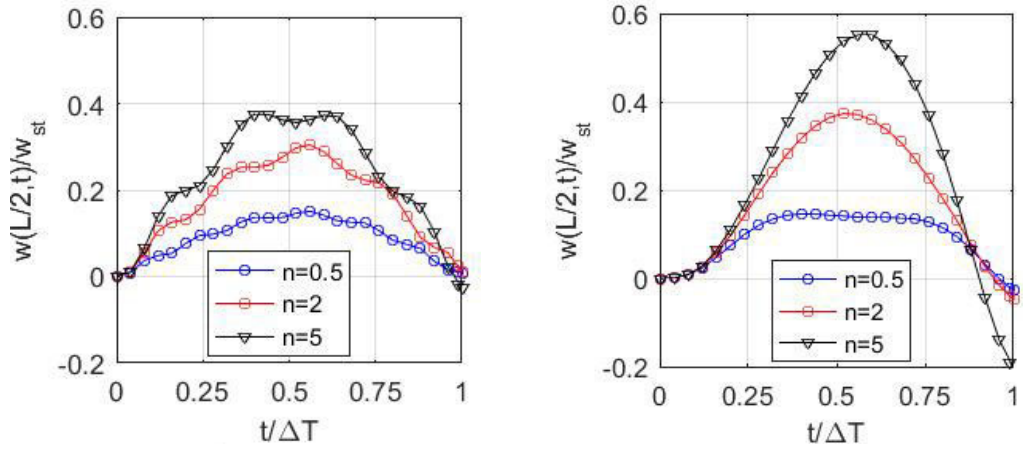

(a) $f_v = 0.1$ (b) $f_v = 0.3$

Figure 4. Time histories for mid-span deflection for $L/h = 20, \eta = 2, r_m = 0.5$, and various values of the power-law index and speed parameter

The variations of the dynamic magnification factor D_d with speed parameter are presented in Figs. 6 and 7 for different values of dimensionless material length scale parameter η and mass ratio r_m, respectively. The figures show that the factor D_d is greatly affected by the speed parameter, the factor

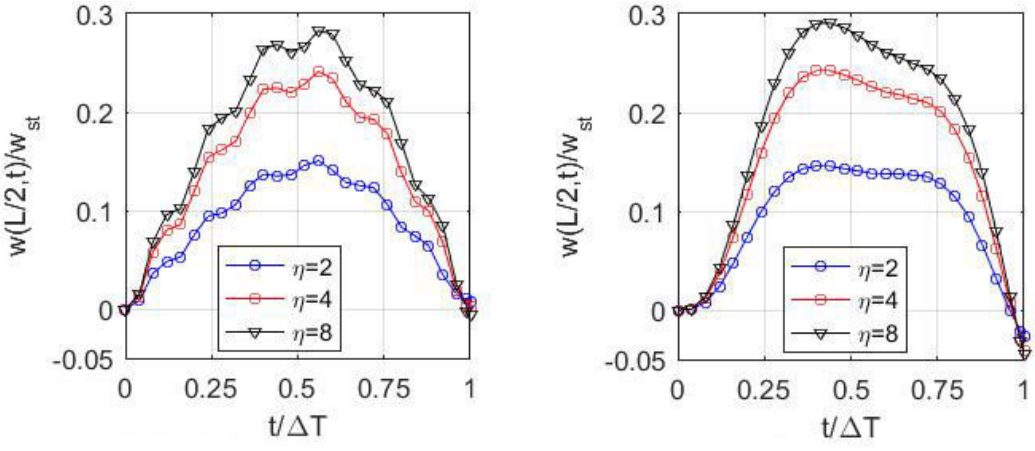

(a) $f_v = 0.1$ (b) $f_v = 0.3$

Figure 5. Time histories for mid-span deflection for $L/h = 20, n = 0.5, r_m = 0.5$, and various values of dimensionless material length scale parameter and speed parameter

D_d repeatedly increases and decreases when the speed parameter increases, and then it approaches the maximum value. The iterative process of increasing and decreasing of $D_d - f_v$ curve is the same for different values of the dimensionless material length scale parameter, Fig. 6, and mass ratio, as seen in Fig. 7. On the other hand, the factor D_d is higher for a higher value of parameter η, see Fig. 6, regardless of the speed parameter. The observation from Fig. 7 shows that the maximum value of D_d is larger for the value of the higher mass ratio.

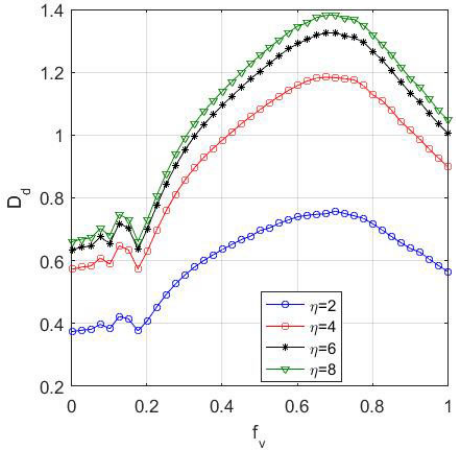

Figure 6. Variation of dynamic magnification factor with speed parameter for $L/h = 20, n = 5, r_m = 0.5$ and various values of dimensionless material length scale parameter

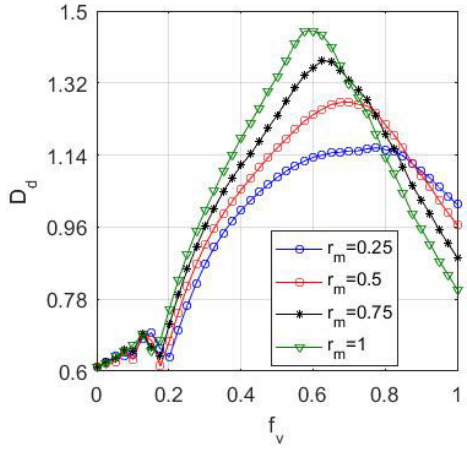

Figure 7. Variation of dynamic magnification factor with speed parameter for $L/h = 20, n = 5, \eta = 5$ and various values of mass ratio

Fig. 8 shows the thickness distribution of normal stress of AFG microbeam for $L/h = 20, n = 0.5, r_m = 0.5, f_v = 0.1$ and various values of the dimensionless material length scale parameter η. The normal stress is normalized by $\sigma_0 = mg/bh$, that is $\sigma^*_{xx} = \sigma_{xx}(L/2, z)/\sigma_0$. It is clear from the figure that the parameter η has a significant effect on the normal stress, increasing the parameter η leads to an increase in the normal stress.

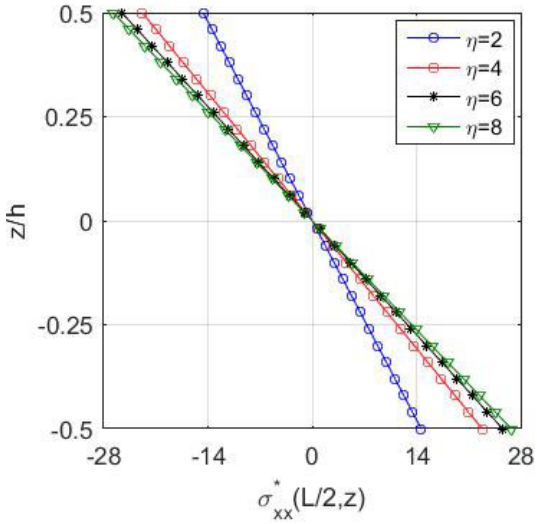

Figure 8. Thickness distribution of normal stress of AFG microbeam for $L/h = 20, n = 0.5, r_m = 0.5, f_v = 0.1$ and various values of dimensionless material length scale parameter

5. Conclusions

The dynamic response of the AFG microbeams under a moving mass has been studied in this paper by using a finite element model. The material properties of the microbeams were assumed to vary in the longitudinal direction by the power-law function and they are evaluated by Mori-Tanaka scheme. Based on the modified couple stress theory and Hamilton's principle, the differential equations of motion for AFG microbeam are established in the framework of the first-order shear deformation beam theory. A two-node beam element with six degrees of freedom was derived and used in conjunction with Newmark method to compute the dynamic responses. Numerical investigations obtained for a simply supported microbeam reveal the importance of the microsize effect on the dynamic response, and the dynamic magnification factor of the microbeam increases with the increase of the material length scale parameter η. The effects of various parameters such as the power-law index, the moving mass speed and the moving mass ratio on the dynamic behavior of the microbeam have been examined in detail and highlighted.

Acknowledgements

This research is funded by University of Transport and Communications (UTC) under grant number T2023-CB-004.

References

[1] Wang, B., Zhao, J., Zhou, S. (2010). A micro scale Timoshenko beam model based on strain gradient elasticity theory. *European Journal of Mechanics-A/Solids*, 29(4):591–599.

[2] Yang, F. A. C. M., Chong, A. C. M., Lam, D. C. C., Tong, P. (2002). Couple stress based strain gradient theory for elasticity. *International journal of solids and structures*, 39(10):2731–2743.

[3] Park, S. K., Gao, X. L. (2006). Bernoulli–Euler beam model based on a modified couple stress theory. *Journal of Micromechanics and Microengineering*, 16(11):2355.

[4] Ma, H. M., Gao, X.-L., Reddy, J. N. (2008). A microstructure-dependent Timoshenko beam model based on a modified couple stress theory. *Journal of the Mechanics and Physics of Solids*, 56(12):3379–3391.

[5] Kahrobaiyan, M. H., Asghari, M., Ahmadian, M. T. (2014). A Timoshenko beam element based on the modified couple stress theory. *International Journal of Mechanical Sciences*, 79:75–83.

[6] Ke, L.-L., Wang, Y.-S. (2011). Size effect on dynamic stability of functionally graded microbeams based on a modified couple stress theory. *Composite Structures*, 93(2):342–350.

[7] Şimşek, M., Reddy, J. N. (2013). Bending and vibration of functionally graded microbeams using a new higher order beam theory and the modified couple stress theory. *International Journal of Engineering Science*, 64:37–53.

[8] Nateghi, A., Salamat-Talab, M. (2013). Thermal effect on size dependent behavior of functionally graded microbeams based on modified couple stress theory. *Composite Structures*, 96:97–110.

[9] Ansari, R., Gholami, R., Sahmani, S. (2011). Free vibration analysis of size-dependent functionally graded microbeams based on the strain gradient Timoshenko beam theory. *Composite Structures*, 94(1): 221–228.

[10] Olsson, M. (1991). On the fundamental moving load problem. *Journal of Sound and Vibration*, 145(2): 299–307.

[11] Wu, J.-J. (2005). Dynamic analysis of an inclined beam due to moving loads. *Journal of Sound and Vibration*, 288(1-2):107–131.

[12] Gan, B. S., Trinh, T.-H., Le, T.-H., Nguyen, D.-K. (2015). Dynamic response of non-uniform Timoshenko beams made of axially FGM subjected to multiple moving point loads. *Structural Engineering and Mechanics, An Int'l Journal*, 53(5):981–995.

[13] Şimşek, M., Kocatürk, T., Akbaş, Ş. (2012). Dynamic behavior of an axially functionally graded beam under action of a moving harmonic load. *Composite Structures*, 94(8):2358–2364.

[14] Ebrahimi-Mamaghani, A., Sarparast, H., Rezaei, M. (2020). On the vibrations of axially graded Rayleigh beams under a moving load. *Applied Mathematical Modelling*, 84:554–570.

[15] Khalili, S. M. R., Jafari, A. A., Eftekhari, S. A. (2010). A mixed Ritz-DQ method for forced vibration of functionally graded beams carrying moving loads. *Composite Structures*, 92(10):2497–2511.

[16] Nguyen, D. K., Nguyen, Q. H., Tran, T. T., Bui, V. T. (2017). Vibration of bi-dimensional functionally graded Timoshenko beams excited by a moving load. *Acta Mechanica*, 228:141–155.

[17] Esen, I., Koc, M. A., Cay, Y. (2018). Finite element formulation and analysis of a functionally graded Timoshenko beam subjected to an accelerating mass including inertial effects of the mass. *Latin American Journal of Solids and Structures*, 15.

[18] Esen, I., Abdelrahman, A. A., Eltaher, M. A. (2020). Dynamics analysis of timoshenko perforated microbeams under moving loads. *Engineering with Computers*, 1–17.

[19] Mori, T., Tanaka, K. (1973). Average stress in matrix and average elastic energy of materials with misfitting inclusions. *Acta Metallurgica*, 21(5):571–574.

[20] Kosmatka, J. B. (1995). An improved two-node finite element for stability and natural frequencies of axial-loaded Timoshenko beams. *Computers & Structures*, 57(1):141–149.